

## FABRICATION OF NOVEL METAL ALLOY FOAMS FOR BIOMEDICAL APPLICATIONS

C.E. Wen<sup>1</sup>, Y. Yamada<sup>2</sup>, P.D. Hodgson<sup>1</sup>

<sup>1</sup> Faculty of Science and Technology, Deakin University, Geelong, 3217, Australia

<sup>2</sup> Materials Research Institute for Sustainable Development, National Institute of Advanced Industrial Science and Technology (AIST), Nagoya, 463-8560, Japan

---

### ABSTRACT

Degeneration of the weight bearing bones of the ageing population often requires the inception of metallic biomaterials. Research in this area is receiving increased attention globally. However, most of today's artificial bone materials are dense and suffer from problems of adverse reaction, biomechanical mismatch and lack of appropriate space for the regeneration of new bone tissues. In the present study, novel ZrTi alloy foams with a porous structure and mechanical properties that are very close to those of bone were fabricated. These ZrTi alloy foams are biocompatible, and display a porous structure permitting the ingrowth of new bone tissues.

---

### 1. INTRODUCTION

Bone injuries and failures often require the inception of implant biomaterials. Research in this area is receiving increased attention throughout the world. Various artificial implant biomaterials, such as metals, polymeric materials and ceramics are being explored to replace the diseased bones [1-3]. However, the traditional implant biomaterials are dense and suffer from problems of adverse reaction, inadequate mechanical properties and lack of capability to induce bone tissue regeneration, shortening the lifetime of the implant biomaterials. Thus, there is an increasing demand to develop new biomaterials in bone tissue engineering, capable of overcoming all or some of these problems.

Research on the biological behavior of metals has shown that the composition of implant biomaterials must be carefully selected to avoid or minimize adverse reactions. The release of metal ions from some metallic implant materials, e.g. Al, Ni, Fe, V and Co, can generate adverse biological effects or elicit allergy reactions [4,5]. On the other hand, investigations have demonstrated that Ti and Zr are favorable non-toxic metals with good biocompatibility [4-6]. Ti, Zr and their alloys are also known as excellent bioactive metallic biomaterials because these alloys can form a bone-like apatite layer on their surfaces in the living body, and bond to bone through this apatite layer [7,8]. Pure Ti and some Ti alloys, e.g. Ti-29Nb-13Ta-4.6Zr [9] and Ti-15Zr-4Nb-2Ta-0.2Pd alloy [10] have already found a wide range of applications in implant biomaterials under loading-bearing conditions. In particular, Zr is a metal with a strong glass-forming ability and bulk amorphous Zr-based alloys exhibit high mechanical strength, high fracture toughness and good corrosion resistance [11]. Therefore, ZrTi alloy has a high biomedical potential due to its unique property combinations of biocompatibility, bioactivity and mechanical property. Nevertheless, solid metallic

implant biomaterials in use today, including Ti, Zr and their alloys, still suffer from the problems of a biomechanical mismatch of the elastic modulus and the intrinsic structural difference. For an implant biomaterial in bone tissue engineering, interconnected porous structure is required to provide necessary space for cell ingrowth and vascularization [12,13]. High porosity and pore size in the range of 200 to 500  $\mu\text{m}$  are desired [14]. The elastic modulus of bone ranges from 0.1 to 20 GPa and the compressive strength ranges from 2 to 200 MPa [15]. The structure and the elastic modulus of implant biomaterials in bone tissue engineering should match those of the bone. The implant biomaterial should be strong enough to tolerate any *in vivo* stresses and physiological loadings that are imposed on them.

Recently, there has been an increasing interest in fabricating porous scaffolds that mimic the architecture of bone; osteoblasts obtained from the patient's hard tissues can be expanded in culture and seeded onto the scaffolds, gradually integrating with the new bone-tissues *in vitro* and/or *in vivo* [16-18]. The scaffolds or three-dimensional foams provide necessary supports for cells to proliferate and maintain their differentiated function, and their architectures define the ultimate shape of the new bone. Several types of scaffold materials, including hydroxyapatite (HA), poly(-hydroxyesters), and natural polymers such as collagen and chitin have been developed for tissue engineering bone and cartilage [19-21]. Various kinds of calcium apatite scaffolds for bone substitutes are currently commercially available and their number is continuously growing. Typical examples are ProOsteon and ProOsteon500R from Interpore Cross International, Inc [22]. These scaffolds consist of hydroxyapatite converted from coral and carbonated hydroxyapatite. These porous bioactive ceramics and polymeric materials promote bone or tissue ingrowth into pores of the implants, thereby allowing rapid return to the physiologically acceptable state of function. However,

these porous bioactive ceramics might fracture if a sudden force is applied to them during the healing stage due to their extremely weak mechanical properties. They are not often applicable in load bearing applications.

Biocompatible metallic foams are novel implant biomaterials in bone tissue engineering [23-24]. They exhibit a porous structure mimicking that of the bone and simultaneously, provide adjustable mechanical properties through altering the porosity [25-28]. However, there is still insufficient research on metallic foams with high porosity for bone tissue engineering. Pure Ti foams with the porosity of about 80% have been successfully fabricated and showed good elastic modulus. However, they might still not be strong enough when compared to cortical bone [24]. Therefore it is crucial to develop new Ti and Zr alloy foams to achieve both high porosity and high strength at the same time. In the present study, a new biocompatible alloy ZrTi was prepared by using a mechanical alloying (MA) process, which is a versatile technique that has been extensively exploited to produce a variety of stable or metastable crystalline, nanocrystalline or amorphous structures [29]. ZrTi foams were fabricated via a powder metallurgical process by using the ZrTi alloy powders prepared by MA. The characteristics of the ZrTi alloy powders and ZrTi foams are characterized and evaluated by using an X-ray diffraction pattern (XRD), and scanning electron microscopy (SEM). The mechanical properties of the ZrTi foams are examined by compressive testing.

## 2. EXPERIMENTAL PROCEDURES

### 2.1 Preparing Amorphous ZrTi Alloy MA

Starting materials were pure elemental powders of zirconium and titanium with reagent purity ( $\geq 99.9\%$ ). The particle size of the elemental Zr and Ti powders is less than  $45\ \mu\text{m}$ . The elemental powders were mixed together thoroughly with the stoichiometric compositions of ZrTi. All powder handlings were performed under a controlled argon atmosphere in a

glove-box. The powder mixture was then subjected to mechanical alloying to synthesize ZrTi alloy. To investigate the evolution of phase formation, various ball milling times such as 180 ks, 360 ks and 720 ks were selected. A Retsch planetary ball milling system with zirconia vials (500ml) and balls ( $\Phi 5\text{mm}$ ) were used for the MA processes. The elemental powder mixtures were sealed into the zirconia vials with a highly purified argon atmosphere at a pressure of 66 kPa during ball milling. The ball milling was performed at a rotation rate of 180 rpm and cooled by an air conditioner. The ball-to-powder weight ratio was controlled at 20:1 and 40 grams of powders were loaded for each run. About 1mass% of stearic acid ( $\text{CH}_3(\text{CH}_2)_{16}\text{COOH}$ ) was used as a process control agent. The amorphization progress and the phases of the mechanically alloyed powders were monitored by XRD and observed by SEM.

### 2.2 Fabricating of ZrTi Foams

A powder metallurgical process was used to fabricate the ZrTi alloy foams. The process consisted of mixing, compacting and heat-treating steps. The illustration of the process from elemental powders is shown in Figure 1 schematically. At first, amorphous ZrTi alloy powders, which were prepared by mechanical alloying, and ammonium hydrogen carbonate particles were blended together in an agate mortar. The ammonium hydrogen carbonate particles were used as a space-holding material in this process. The particle size ranged from 200 to  $500\ \mu\text{m}$  for the space-holding material, and was carefully sieved to ensure that the finishing ZrTi foams exhibited a porous structure with pore size ranging from 200 to  $500\ \mu\text{m}$ . The green compacts were then processed by compacting at a pressure of 200MPa. Then they were then heat-treated to burn-out the space-holding particles and to sinter ZrTi foam samples. A vacuum furnace was used for the heat treatments. The heat-treatment process was performed at  $200^\circ\text{C}$  for five hours to burn-out the space-holding material and at  $1300^\circ\text{C}$  for 2 hours to sinter the ZrTi foams. ZrTi foams with a relative density of 0.30 were fabricated.

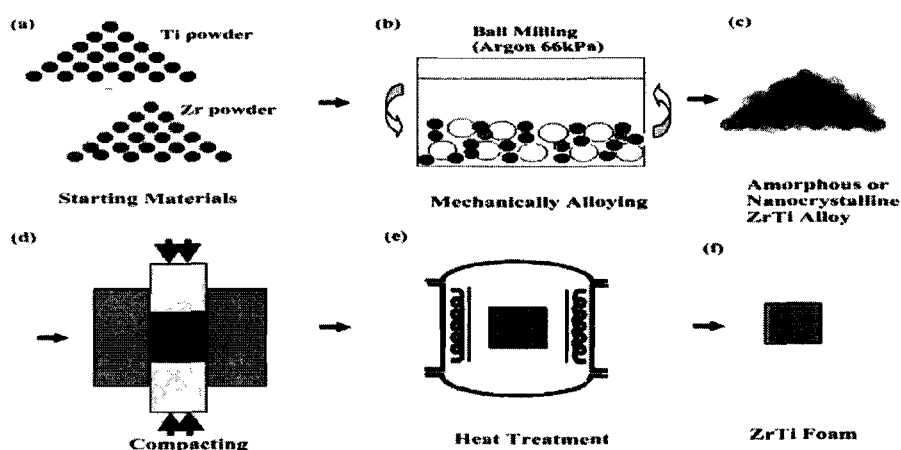


Figure 1: Schematic illustration of the fabrication process for ZrTi foams

### 2.3 Characterization and Evaluation for the ZrTi Foam

In the present study, cylindrical ZrTi foam samples were fabricated for examining the macro- and micro-structural characteristics and the mechanical properties. X-ray diffraction patterns and scanning electron microscopy (SEM) were used to characterize the ZrTi alloy foam samples. Quantitative image analyses by using Image-Pro Plus software were conducted to measure the pore size distribution. A compression test was carried out on the foam sample ( $\Phi 12 \times 15$  mm) at room temperature with an initial strain rate of  $10^{-3} \text{ s}^{-1}$  to determine the mechanical properties.

## 3. RESULTS AND DISCUSSION

### 3.1 Amorphous ZrTi alloy Prepared by Mechanical Alloying

The mixture of elemental Zr powder and Ti powder with the stoichiometric compositions of ZrTi was mechanically alloyed for different times of 180ks, 360ks and 720ks. The X-ray diffraction patterns for the initial powders, the MA powders and the MA powders after heat treatment at  $1300^\circ\text{C}$  for 2 hours are shown in Figure 2. The diffraction patterns for the initial powders show sharp peaks belonging to Zr and Ti powders, as shown in Figure 2(a) and (b), respectively. After 180 ks

of ball milling, the diffraction pattern consists of broadened peaks stemming from the amorphous phase of ZrTi alloy, and also sharp peaks tracking the remaining starting crystalline elements of Zr and Ti, as shown in Figure 2(c). It should be noted that a broadening of the individual reflexes can be observed because of the decrease in grain size and the increase of the amount of deformation (Figure 2(c)). With the increasing of the milling time to 360 ks, the amount of amorphous phase increases distinctly. In addition, the intensities of the crystalline diffraction peaks are dramatically reduced compared to that of the powders after 180 ks ball milling and Ti is no longer detectable as shown in Figure 2(d). After 720 ks of ball milling only a typical broad maximum of an amorphous phase is visible as shown in Figure 2(e). This diffraction pattern indicates the complete amorphous phase of ZrTi alloy and shows no tracks of elemental crystalline Zr and Ti powders. Figure 2(f) shows the diffraction pattern for the stoichiometric ZrTi powders after 720 ks of ball milling and subsequently heat treatment at  $1300^\circ\text{C}$  for 2 hours. It can be seen that the amorphous phase of ZrTi alloy crystallized completely after the heat treatment. Observations by scanning electron microscopy (SEM) found that the particle size of the stoichiometric ZrTi powders after 720 ks mechanical alloying is less than  $7\mu\text{m}$ , as shown in Figure 3. The particle size of the MA powders was reported to critically affect the density, hardness, and microstructure of the final sintered product [30].

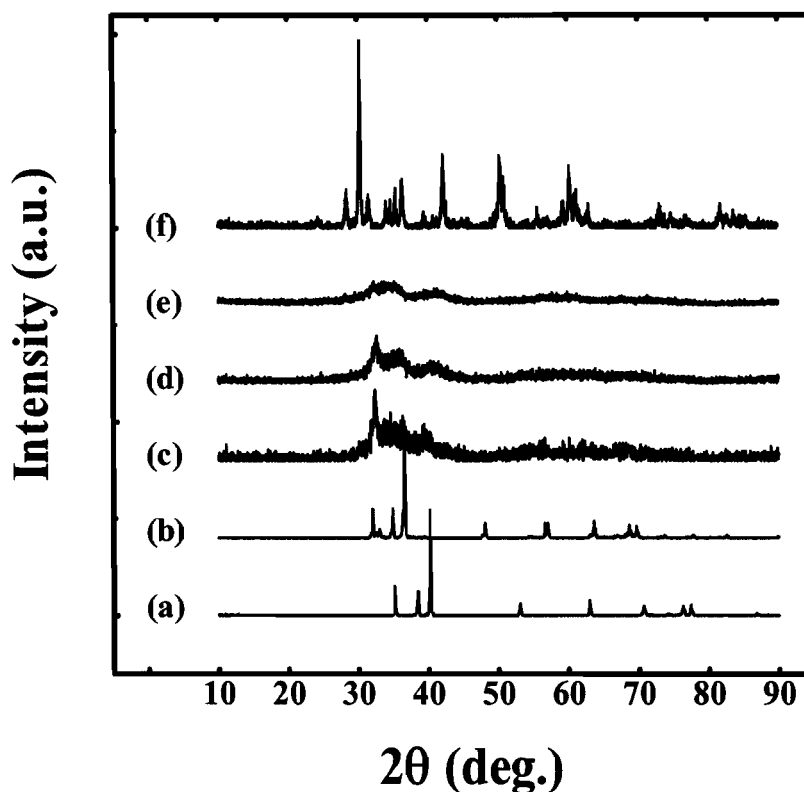


Figure 2: The XRD patterns of the ZrTi powders after various periods of mechanical alloying (a) Ti powders, MA 0ks; (b) Zr powders, MA 0ks; (c) Stoichiometric ZrTi powders, MA 180ks; (d) Stoichiometric ZrTi powders, MA 360ks; (e) Stoichiometric ZrTi powders, MA 720ks; (f) Stoichiometric ZrTi powders, MA 720ks and subsequently heat treated at  $1300^\circ\text{C}$  for 2 hr.



Figure 3: Scanning electron micrograph of the amorphous ZrTi particles (MA 720ks).

### 3.2 ZrTi foams fabricated by using the mechanically alloyed powders

#### 3.2.1 Microstructural characteristics

Figure 4 shows the SEM micrograph of the ZrTi foam sample with a relative density of 0.30. Microstructural observations revealed that the ZrTi foam sample exhibited a bimodal porous structure, *i.e.* macropores and micropores. The macropores of the ZrTi alloy foam were interconnected throughout the whole sample and their sizes lay between 200 - 500  $\mu\text{m}$ . The pore size for the macropores was specifically tailored for the ingrowth of the new bone tissues [14]. In addition, the ZrTi foam displayed another kind of pore, *i.e.* micropores, which were distributed at the cell edges of the macropores. The micropores had a size of only several microns. Such micropores permit body fluid communication and nutrient transport.

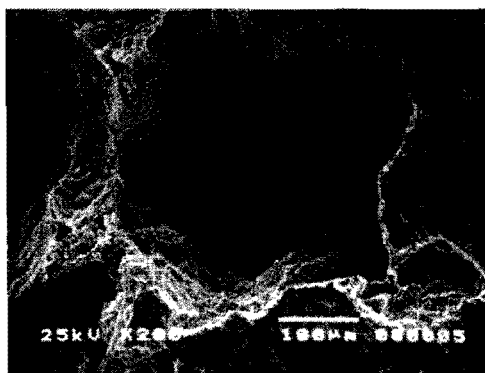


Figure 4: SEM micrograph showing the porous structure of the ZrTi foam.

#### 3.2.2 Mechanical properties

A compressive test was performed on the ZrTi foam sample with a relative density of 0.3. The nominal stress - nominal strain curve for the ZrTi foam sample is shown in Figure 5. It can be seen that the ZrTi foam showed the typical deformation behavior of metallic foams under compressive loading [31]. The nominal stress - nominal strain curve can be divided into three regions, that is, an elastic deformation region at the beginning of deformation, a plateau region with a nearly constant flow stress to a large strain, and a

densification region where the flow stress increases rapidly. The compressive plateau stress and the Young's modulus of the ZrTi foam were 78.4 MPa and 15.3 GPa, respectively. To achieve a functionally satisfying implant in practical applications, porous scaffold design needs to consider both the strength and the Young's modulus. The elastic modulus of bone ranges from 0.1 to 20 GPa; and the compressive strength ranges from 2 to 200 MPa [15]. The elastic moduli of bone and implants should be as similar as possible to avoid stress shielding and concentration effects, which may lead to bone resorption and even necrosis. It can be seen that the mechanical properties of the ZrTi foam were very close to those of the natural bone. However, the mechanical properties of natural bones are different depending on some factors such as the type, age, gender, and race. Therefore, the mechanical property requirements for the implant materials change accordingly. Further research is needed to cope with the detailed requirements for each implant material to match those of the bone.

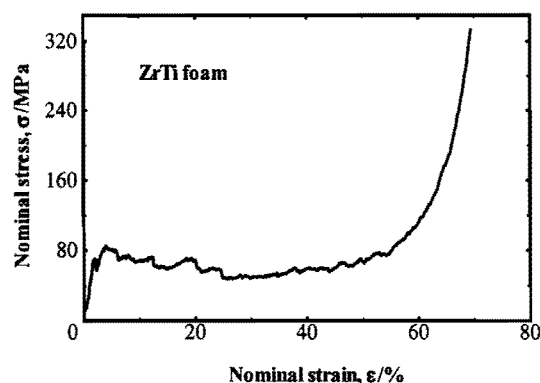


Figure 5: Nominal stress - nominal strain of the ZrTi foam.

## 5. CONCLUSIONS

ZrTi foams were fabricated by using amorphous ZrTi alloy powders that were prepared by mechanical alloying. The main results are as follows.

1. Mechanical alloying of the elemental powders of stoichiometric ZrTi led to the formation of an amorphous ZrTi alloy.
2. The amount of the amorphous phase increased with an increase in the ball milling time. A complete amorphous phase of ZrTi alloy with a fine particle size of less than 7  $\mu\text{m}$  was obtained after 720 ks mechanical alloying.
3. ZrTi foams were fabricated by using the amorphous ZrTi alloy powders. The heat treatment was performed at a temperature of 1300  $^{\circ}\text{C}$  and held for 2 hours.
4. Both the porous structure and the mechanical properties of the ZrTi foam were close to that of natural bone.